



## Original article

# A new method for clastic reservoir prediction based on numerical simulation of diagenesis: A case study of Ed<sub>1</sub> sandstones in Bozhong depression, Bohai Bay Basin, China

Wendao Qian<sup>1</sup>, Taiju Yin<sup>1</sup>\*, Guowei Hou<sup>2</sup>

<sup>1</sup>School of Geoscience, Yangtze University, Wuhan 430100, P. R. China

<sup>2</sup>Shanghai Branch of CNOOC Ltd., Shanghai 200030, P. R. China

(Received November 12, 2018; revised December 10, 2018; accepted December 11, 2018; available online December 19, 2018)

### Citation:

Qian, W., Yin, T., Hou, G. A new method for clastic reservoir prediction based on numerical simulation of diagenesis: A case study of Ed<sub>1</sub> sandstones in Bozhong depression, Bohai Bay Basin, China. *Advances in Geo-Energy Research*, 2019, 3(1): 82-93, doi: 10.26804/ager.2019.01.07.

### Corresponding author:

\*E-mail: [yintaij@yangtzeu.edu.cn](mailto:yintaij@yangtzeu.edu.cn)

### Keywords:

Clastic reservoir  
diagenetic simulation  
diagenetic stages  
diagenetic facies  
porosity

### Abstract:

The use of seismic exploration technique to provide reliable reservoir information is a conventional method. However, due to its quality and resolution reasons, it cannot satisfy the detailed research and characterization of reservoirs, especially the clastic reservoir with thin sand body. Diagenesis is a fundamental process in the development and formation of all petroleum reservoirs and is a major contributor to their ultimate physical properties. Based on numerical simulation of diagenesis, a new prediction method called geology prediction techniques is presented to simulate the evolution of the diagenetic stages, diagenetic facies and porosity of clastic reservoirs and ultimately for favorable reservoir prediction. It emphasizes the idea of dynamic quantitative research dominated by process recovery, the most important of which is the establishment of mathematical models, including mineral dissolution models, mineral cementation models and sediment compaction models using the experimental data in study area and the results of previous studies. The essence of this method is illustrated, and its effectiveness is proved using Ed<sub>1</sub> clastic sandstones in the Bozhong depression, Bohai Bay Basin, China. At present, the reservoir is in the early diagenetic stage B (IB) and the middle diagenetic stage A1 (IIA1). The major diagenetic processes that influence the porosity of the sandstones in study area are mechanical compaction, carbonate cementation, quartz cementation, clay cementation, feldspar dissolution and carbonate dissolution. There are three types of sandstones including fine sandstone, siltstone, and argillaceous siltstone, and the variation range of primary porosity of these sandstones is from 26% to 38%. Compaction and carbonate cementation are the main reasons for porosity reduction, with porosity loss percentage by compaction (P-Com) and porosity loss percentage by cementation of carbonate (P-C-Car) being 53.1% ~ 7.8% (av. 41.9%) and 53.1% ~ 7.8% (av. 18%), respectively, while carbonate dissolution and feldspar dissolution can greatly improve reservoir physical property, with porosity increase percentage by dissolution of carbonate (P-D-Car) and porosity increase percentage by dissolution of feldspar (P-D-Fel) being 0 ~ 9.9% (av. 8.9%) and 0 ~ 27.8% (av. 9.4%), respectively. The predicted porosities match the measured porosities well.

## 1. Introduction

Reservoir porosity and permeability are critical parameters for oil and gas exploration and production. Most previous attempts at reservoir quality prediction have relied on physical simulation or numerical simulation after empirical correlations to understand the variation laws of the physical properties of sandstone reservoirs in the process of diagenesis (Wood and Byrnes, 1994). The compaction-tectonic subsidence models in sedimentary basin are constructed (Marc et al., 1993; David et al., 2001). Based on dynamic equations and thermodynamic

equations, models of single mineral diagenesis are established and used to calculate dissolution or cementation percentage (Walderhaug, 1996; Lander et al., 1999; Meng, 2013; Randolph et al., 2015). The simulation experiments of sandstone diagenesis including compaction, cementation and dissolution are a function of time and depth. However, most of these models connect directly with diagenesis intensity over time or depth rather than porosity variation.

The relationship between the porosity of sandstone and the buried depth, and the relationship between the porosity and



<https://doi.org/10.26804/ager.2019.01.07>.

2207-9963 © The Author(s) 2019. Published with open access at Ausasia Science and Technology Press on behalf of the Division of Porous Flow, Hubei Province Society of Rock Mechanics and Engineering.

buried time in sedimentary basins give an indication of the effects of depth and burial time on the evolution of porosity for the classic rocks. However, the porosity-permeability-buried depth or porosity-permeability-buried time relationship is non-linear, especially in reservoirs with high diagenesis.

In this research, quantitative mathematical equation models between the destructive and constructive diagenesis and pore evolution are given using the experimental data and the results of previous studies, while coefficients is taken into consideration for different diagenetic strengths in different diagenetic stages. The stronger the diagenesis, the bigger the coefficients is. Finally, based on the quantitative equations, pore evolution in burial history is simulated. On the determination of the diagenetic stages, temperature ( $T$ ), vitrinite reflectivity ( $R_o\%$ ) and their relative weight for reservoir diagenetic stages prediction is taken into consideration, while data in individual wells are taken as constraint condition for diagenetic stages inversion calculation (Fig. 1).

## 2. Materials and methods

### 2.1 Geological setting and samples

Bozhong depression is the largest one in Bohai Basin, with a total area of about 8000 km<sup>2</sup>. The basin is filled with Cenozoic sediments including the Kongdian (Ek), Shahejie (Es), Dongying (Ed), Guantao (Ng), Minghuazhen (Nm) and Pingyuan (Qp) formations. The Dongying formation (Ed) division from the base to the top is the third member of Dongying formation (Ed<sub>3</sub>), the second member of Dongying formation (Ed<sub>2</sub>) and the first member of Dongying formation (Ed<sub>1</sub>), respectively. The tectonic evolution of the basin consists of a synrift stage (65.0 to 24.6 Ma) and a postrift stage (24.6 Ma to the present), and Ed<sub>1</sub> reservoir sedimentation period is from about 29.7 Ma to 28.1 Ma (Lampe et al., 2012). The target interval (Ed<sub>1</sub>) is mainly composed of feldspar quartz sandstone, a few feldspar lithic quartz sandstone, and feldspar lithic sandstone.

### 2.2 Geology prediction technique

Diagenesis is a necessary process for the development and formation of all reservoirs, which ultimately determines the reservoir physical property (Qian, 2017). The geology prediction technique simulates pores evolution and finally predict favorable reservoir through synthetical consideration of primary porosity, diagenetic field and diagenetic process (Fig. 2, Fig. 5).

#### 2.2.1 Primary porosity and diagenetic stages

The research on the evolution of sandstone porosity is the indispensable basis for the analysis of diagenesis evolution, and accurate acquirement of the primary porosity is the basic

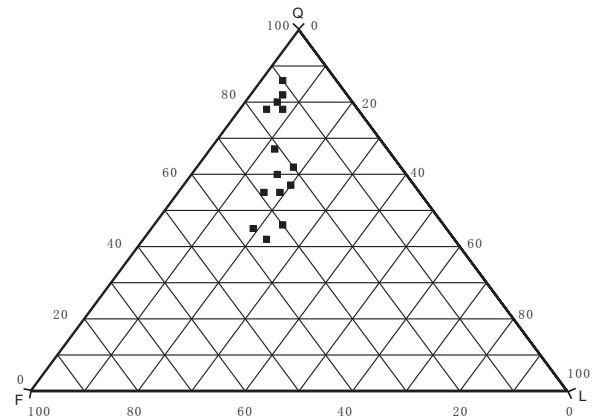


**Fig. 1.** The composition of the Ed<sub>1</sub> clastic sandstones in the Bozhong depression.

prerequisite to achieve the aim. An investigation for the relations among porosity, permeability, and texture of artificially mixed and packed sand has been studied (Beard and Weyl, 1973; Scherer, 1987; Xu et al., 2018). To characterize the characteristics of microfacies (MF), rock types (RT) and rock structures (RS), this study introduce a structural phase parameter (SPP). To unify the factors that affect the original porosity, one parameter is used. Then the model between the primary porosity and SPP to predict the primary porosity ( $V_{primary}$ ) by Eq. (1) and Eq. (2) is established. The primary porosity has positive relationships with grain size and sorting and have negative relationships with matrix contents.

$$f(SPP) = f(MF, RT, RS) \quad (1)$$

$$V_{primary} = f(SPP) \quad (2)$$

Eq. (3) is Beard and Weyl's method. In this model,  $RS$  is used to calculate primary porosity.

$$V_{primary} = 20.91 + \frac{22.9}{S_o} \quad (3)$$

where  $V_{primary}$  is primary porosity;  $S_o$  is sorting coefficient.

It is now evident that diagenesis of clastic rock and hydrocarbon generating capacity have close relationship with diagenetic stages, and thus research on diagenetic process has important significance for petroleum exploration and development (Wilson et al., 1994; Ajdukiewicz et al., 2010; Mahmud et al., 2018). In the sediment burial and diagenesis process, diagenetic fields and diagenetic materials vary with diagenetic stages and exerts great effect on the properties of clastic rock.

Diagenetic stages of clastic strata refers to different evolution phases in the geologic history, and its accurate examining in research area could help us find the favorable region (Meng et al., 2008; Ajdukiewicz et al., 2010). Research on geological indexes and their combined features, mainly including paleo temperature, pore type and its contact relationship, organic characteristics and mineral features, diagenetic stages of clastic strata reservoir for different evolution phases in the geologic

**Table 1.** Characteristics of the samples of fine sandstone, siltstone and argillaceous siltstone in Ed<sub>1</sub> reservoir.

Well	Dep(m)	$\phi$ (%)	Com(%)	D-Fel(%)	D-Car(%)	C-Clay(%)	C-Que(%)	C-Car(%)	SF	DS	RT	$S_o$	Qua(%)
Z1	2870	11.1	47.9	13.4		14.0	4.2	16.2	B	IIA1	FS	1.55	60
Z2	2952	4.8	34.8		7.4	28.0		30.4	B	IIA1	AS	1.81	86
Z3	2905	5.9	53.1			28.0			B	IIA1	AS	2.25	55
Z4	2905	13.6	35.9	4.1	6.3	16.3	3.5	17.7	B	IIA1	FS	1.44	78
Z5	1692	25.3	34.2	15.5		8.0	5.6		A	IB	FS	1.39	42
Z6	1805	15.7	46.0	13.4	59.9	14.8		65.9	A	IB	FS	1.79	62
Z7	1955	4.3	48.3			15.8		22.4	A	IB	SS	2.12	67
Z8	2084	20.2	35.5	6.0		10.4	7.3		A	IB	FS	1.32	82
Z9	2288	16.3	50.0	25.3		17.2	3.4	7.8	B	IIA1	SS	1.65	45
Z10	2279	13.94	27.8	9.6		10.9		32.8	B	IIA1	FS	1.46	55
Z11	2808	1.2	49.2			46.2			B	IIA1	AS	4.51	80
Z12	2414	14.8	43.2	10.3		11.6		15.4	B	IB	SS	1.42	57
Z13	2324	17.29	46.1	27.0		16.3	16.0		A	IB	SS	1.56	46
Z14	2072	21.9	34.9	7.8	18.3	7.8		22.7	A	IB	FS	1.51	78

**Note:** Com is porosity compaction loss percentage; D-Fel is porosity increase percentage by feldspar dissolution; D-Car is porosity increase percentage by carbonate dissolution; C-Clay is porosity loss percentage by clay cementation; C-Que is porosity loss percentage by quartz cementation; C-Car is porosity loss percentage by carbonate cementation; SF is sedimentary facies, A-delta plain, B-delta front; DS is diagenetic stages, IB-Early diagenetic stage B; IIA1-Middle diagenetic stage A1;  $S_o$  is sorting coefficient; Qua is quartz percentage in sandstone.

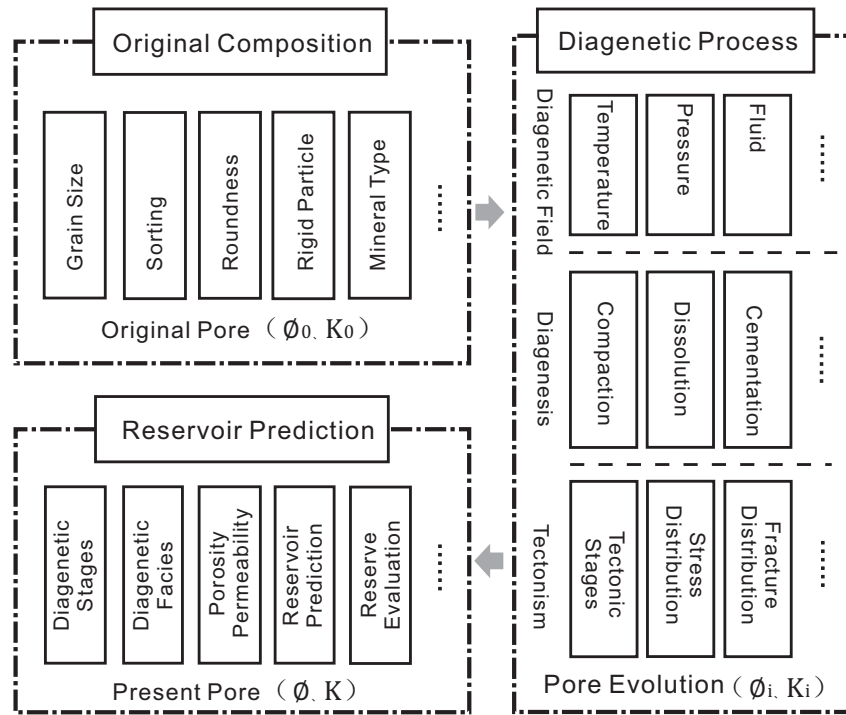


**Fig. 2.** Research ideal about geology prediction technique.

**Table 2.** Division of diagenetic stages in clastic rocks.

Diagenetic stages	Paleo temperature/°C	Pore type & grain contact relationship	$R_o/\%$	$T_{max}/°C$	TAI	I/S-S%	
I	A	> 25-65	Primary pores, point contact	< 0.35	< 430	< 2.0	> 70
	B	> 65-85	Primary pores, secondary pores, point-line contact	0.35-0.5	430-435	2.0-2.5	50-70
II	A1	> 85-110	Dissolution pore and moldic pore, line contact	0.5-0.95	435-450	2.5-3.1	35-50
	A2	> 110-140	Dissolution pore and moldic pore, line contact	0.95-1.3	450-460	3.1-3.7	15-35
	B	> 140-175	Crack, dissolution pore, line and suture line contact	1.3-2.0	460-490	3.7-4.0	< 15
III	> 175-200	Crack, line and suture contact	2.0-4.0	> 490	> 4.0	≈ 0	

**Note:** IA-Early diagenetic stage A; IB-Early diagenetic stage B; IIA1-Middle diagenetic stage A1; IIA2-Middle diagenetic stage A2; IIB-Middle diagenetic stage B; III-Late diagenetic stage.

history is conducted (Ying et al., 2003). It consists of syndiagenetic stage, early diagenetic stage (stage A and stage B of early diagenesis, IA and IB, respectively), middle diagenetic stage (stage A1, stage A2 and stage B of middle diagenesis, IIA1, IIA2 and IIB, respectively), late diagenetic stage (III) and epidiagenetic stage (Table 1). The simulation results of diagenetic stages can be different when choosing different indicators. Based on the comprehensive analysis of previous studies, temperature ( $T$ ), vitrinite reflectivity ( $R_o\%$ ) and their relative weight are considered for Ed<sub>1</sub> reservoir in Bozhong depression stages simulation.

### 2.2.2 Diagenesis and diagenetic facies

Diagenetic facies is a product of both diagenesis and diagenetic stages under the effect of tectonics, which includes rock particles, dissolution, cementation, fabric, pores and cracking. A naming scheme for diagenetic facies is proposed, such as low porosity and low porosity-coarse grained feldspar lithic sandstone-feldspar dissolution facies, which reflects lithology, diagenesis and pore permeability when diagenetic facies is divided (Zhou, 2008). This method can describe in detail the reservoir characteristics, but it is not convenient for practical application. In essence, diagenetic facies is the sum of petrology, geochemistry and rock physics that reflect the diagenetic environment. The naming of diagenetic facies emphasizes diagenesis and diagenesis in the diagenetic environment is proposed (Chen, 1994; Zhong, 1997; Du et al., 2006). A method taking lithology and main diagenesis into consideration describes diagenetic facies as “sandstone-cementation facies”, while single factor diagenetic facies emphasizes the main diagenesis, for example, quartz secondary increase diagenetic facies. Because of the complexity of diagenesis, it is difficult to avoid the one-sided description of reservoir diagenetic characteristics for single factor diagenetic facies. Some methods emphasize the diagenesis and diagenetic process, naming the diagenetic facies with important diagenesis that determines the physical characteristics of the reservoir, such as medium strong dissolving-middle glue formation facies (Grigsby et al., 1996; Elfegh et al., 1999; Xia et al., 2012). Sedimentary-diagenetic facies takes sedimentary facies and diagenesis into consideration, and its identification is using logging data by the use of the discriminant analysis and corresponding crossplots

(Wang et al., 2017). In this study, a new method to describe pores evolution using Eqs. (4) - (10) was proposed through synthetical consideration of diagenesis including mechanical compaction, quartz cementation, carbonate cementation, clay cementation, feldspar dissolution and carbonate dissolution and their strength in different diagenetic stages for porosity simulation. This method is connected directly with porosity variation over time or depth rather than diagenesis intensity.

On the determination of the diagenetic stages, parameters including paleo temperature ( $T$ ), vitrinite reflectivity ( $R_o\%$ ), the highest pyrolysis peak temperature ( $T_{max}$ ), thermal alteration index (TAI) and the proportion of smectite in illite/smectite interstratified minerals ( $I/S - S\%$ ) can be used for reservoir diagenetic stages division (Table 2).

$$P - Com = \frac{V - Compaction}{V_{primary}} \times 100\% \quad (4)$$

$$P - C - M = \frac{V - M - Cementation}{V_{primary}} \times 100\% \quad (5)$$

$$P - D - M = \frac{V - M - Dissolution}{V_{primary}} \times 100\% \quad (6)$$

$$V_{primary} = 20.91 + \frac{22.9}{S_o} \quad (7)$$

$$R - Com = \frac{P - Com}{t} \quad (8)$$

$$R - C - M = \frac{P - C - M}{t} \quad (9)$$

$$R - D - M = \frac{P - D - M}{t} \quad (10)$$

where  $V_{primary}$  is primary pore volume, %;  $V - Compaction$  is the pore volume destroyed by compaction, %;  $V - M - Cementation$  is cementation pore volume by single mineral, %;  $V - M - Dissolution$  is dissolution pore volume by single mineral, %;  $P - Com$  is porosity loss percentage by compaction, %;  $P - C - M$  is porosity loss percentage by cementation of single mineral, %;  $P - D - M$  is porosity increase percentage by dissolution of single mineral, %;  $S_o$  is sorting coefficient;  $R - Com$  is porosity loss percentage by

compaction in per unit time,  $\text{Ma}^{-1}$ ;  $R - C - M$  is porosity loss percentage by cementation of single mineral in per unit time,  $\text{Ma}^{-1}$ ;  $R - D - M$  is porosity increase percentage by dissolution of single mineral in per unit time,  $\text{Ma}^{-1}$ ;  $t$  is diagenesis time,  $\text{Ma}$ .

### 2.2.3 Diagenesis and pores evolution

#### (A) Compaction

It has been shown that mechanical compaction is one of the main reasons for the large reduction of primary pores in the sand body. The existence of compaction has greatly reduced the primary intergranular pores, and the compaction reduction rate in some places can reach more than 50%, which greatly affects the reservoir property of the sand body. The main controlling factors for mechanical compaction are pressure intensity, composition and sorting of sediments. From the factors affecting the compaction, geological factors including buried depth, geological age, thermal maturity, temperature, deposition rate, quartz content, cementation degree on compaction are considered. A depth-dependent exponential function to study the relationship between mechanical compaction and pores evolution is established (David, 1999).

$$V_{\text{Com}} = \partial_1 \left( \frac{e^{-cg(\rho_s - \rho_w)z}}{e^{-cg(\rho_s - \rho_w)z} + k_1} \right) \quad (11)$$

where  $k_1 = (1 - \phi_0)/\phi_0$ ;  $\rho_s = 2650 \text{ kg/m}^3$ ;  $\rho_w = 1.0 \times 10^3 \text{ kg/m}^3$ ;  $c = 3.68 \times 10^{-8} \text{ Pa}^{-1}$ ;  $g = 9.8 \text{ N/kg}$ ;  $z$  is burial depth;  $V_{\text{Com}}$  is the volume destroyed by compaction, and  $\partial_1 = 1.2$ ,  $\partial_1 = 1.0$ ,  $\partial_1 = 0.75$  represent strong compaction, middle compaction and weak compaction, respectively.

#### (B) Cementation

The cement types in the  $\text{Ed}_1$  sandstone reservoirs in the Bozhong depression consist mainly of carbonates, authigenic quartz and clay minerals (Table 1). Carbonate cement has the highest content and mainly fills primary intergranular pores and dissolution pores. The negative influence on reservoir physical property of the carbonate cements (calcite and dolomite) is much bigger than that of the cement that surrounds grains (e.g., quartz overgrowths and authigenic clay). The porosity loss percentage of carbonate cements and authigenic quartz in the  $\text{Ed}_1$  sandstones are 7.8% ~ 65.9% (av. 25.7%) and 0 - 16% (av. 6.7%), respectively. The clay in the  $\text{Ed}_1$  sandstones mainly includes clay matrix and authigenic clay minerals, and the latter formed during diagenetic processes. The XRD result indicates that the porosity loss percentage of clay cement in the  $\text{Ed}_1$  sandstones is ranging from 7.8% and 46.2%, with an average of 17.5%.

The effect of destructive diagenesis on pores in burial history using models including Olac Walderhaug model for quartz cementation calculation (Eq. (12)), numerical fitting models for clay cementation calculation (Eq. (13)) and carbonate cementation calculation is calculated (Eq. (14)). The equations of adsorption thermodynamics and adsorption kinetics to describe carbonate and clay cementation characteristics have been used (Tribble et al., 1995; Meng et al., 2006; Jin et al., 2009), but carbonate and clay cementation percentage with time or depth in previous studies is not. Thus, new methods to discuss their

effect on pores evolution based on individual well data in study area are used (Fig. 3, Fig. 4).

$$V_{\text{Qua\_Cem}} = \partial_2 (V_{q2} - (\Phi_0 - (\Phi_0 - V_{q1})) \times \exp \frac{-MaA_0}{\rho\Phi_0bc \ln 10} (10^{bT_2} - 10^{bT_1})) \quad (12)$$

where  $a = 1.98 \times 10^{-22} \text{ moles/cm}^2\text{s}$ ;  $b = 0.022 \text{ }^\circ\text{C}^{-1}$ ;  $M$  is the molar mass of quartz (60.09 g/mole);  $\rho$  is the density of quartz (2.65 g/cm<sup>3</sup>);  $T$  is reaction temperature ( $^\circ\text{C}$ );  $V_{q2}$  is the amount of quartz cement (cm<sup>3</sup>) precipitated from time  $T_1$  to  $T_2$ ;  $V_{q1}$  is the amount of quartz cement present at time  $T_1$ ;  $A_0$  is initial quartz surface area;  $\partial_2$  is cementation strength, and  $\partial_2 = 1.2$ ,  $\partial_2 = 1.0$ ,  $\partial_2 = 0.75$  represent strong quartz cementation, middle quartz cementation and weak quartz cementation, respectively.

$$V_{\text{Clay\_Cem}} = \partial_3 (1.478 \times 10^{-12} X^4 - 1.012 \times 10^{-8} X^3 + 1.708 \times 10^{-5} X^2 + 1.617 \times 10^{-3} X + 0.2806) \quad (13)$$

where  $X$  is burial depth, m;  $V_{\text{Clay\_Cem}}$  is porosity destroyed by clay cementation.  $\partial_3$  is cementation strength, and  $\partial_3 = 2$ ,  $\partial_3 = 1.0$ ,  $\partial_3 = 0.5$  represent strong clay cementation, middle clay cementation and weak clay cementation, respectively.

$$V_{\text{Car\_Cem}} = \partial_4 (7.39 \times 10^{-13} X^4 - 5.06 \times 10^{-9} X^3 + 8.54 \times 10^{-6} X^2 + 8.085 \times 10^{-4} X + 0.00805) \quad (14)$$

where  $X$  is burial depth, m;  $V_{\text{Car\_Cem}}$  is porosity destroyed by carbonate cementation.  $\partial_4$  is cementation strength, and  $\partial_4 = 2$ ,  $\partial_4 = 1.0$ ,  $\partial_4 = 0.5$  represent strong carbonate cementation, middle carbonate cementation and weak carbonate cementation, respectively.

#### (C) Dissolution

Dissolution in the  $\text{Ed}_1$  sandstones mainly occurred in feldspars and carbonate. The porosity increase percentage of feldspars in the fine sandstone, siltstone and argillaceous siltstone are 4.1% ~ 15.5% (av. 9.9%), 0% ~ 27.0% (av. 15.6%), and 0%, respectively, while the porosity increase percentage of carbonate in the fine sandstone, siltstone and argillaceous siltstone are 0% ~ 59.9% (av. 22.9%), 0%, and 0% ~ 7.4% (av. 2.5%), respectively.

The effect of constructive diagenesis on pores in burial history is calculated using models including Pan Gaofeng's model for feldspar dissolution calculation (Eq. (15)) and Craig's model for quartz dissolution calculation (Eq. (16)). Because carbonate dissolution percentage with time or depth have not been discussed in previous studies, new methods are used to discuss their effect on pores evolution based on individual well data in study area (Fig. 3, Fig. 4, Eq. (17)).

$$V_{\text{Fel\_Dis}} = \partial_5 \left( \frac{2\Delta\phi}{\Delta t^3} (t - t_1)^3 + \frac{3\Delta\phi}{\Delta t^2} (t - t_1)^2 \right) \quad (15)$$

where  $t$  is reaction time,  $\text{Ma}$ ;  $\Delta\phi$  is porosity variation, %;  $t_1$  is temperature at 70  $^\circ\text{C}$  for the first time,  $\text{Ma}$ ;  $t_2$  is temperature at 90  $^\circ\text{C}$  for the first time,  $\text{Ma}$ ;  $\Delta t = t_1 - t_2$ ;  $V_{\text{Fel\_Dis}}$  is po-

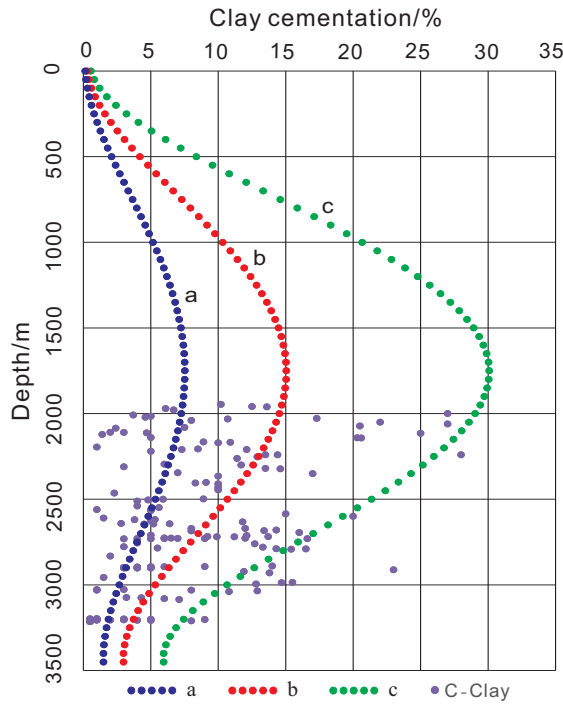


**Fig. 3.** Percentage composition of clay mineral in the vertical direction and nonlinear curve fitting to analyzing the experiment data. Curve a represents weak clay cementation; Curve b represents middle clay cementation; Curve c represents strong clay cementation.

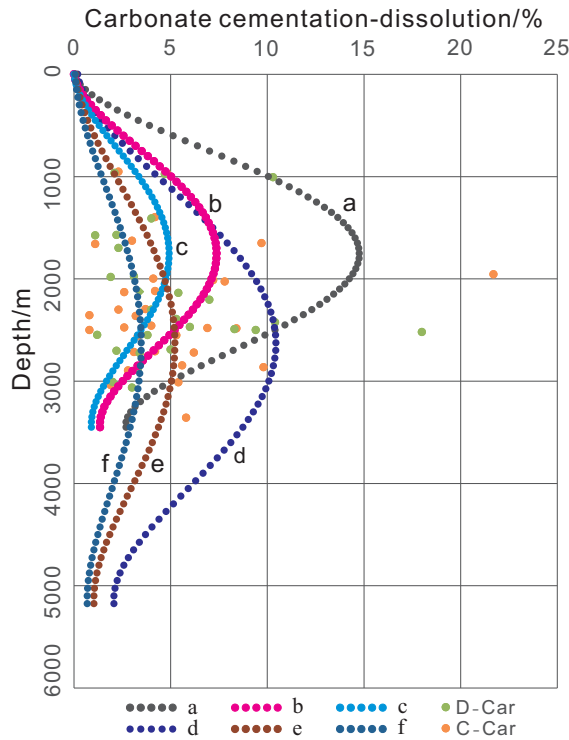


**Fig. 4.** Percentage composition of carbonate cementation and dissolution in the vertical direction and nonlinear curve fitting to analyzing the experiment data. Curve a represents strong carbonate cementation; Curve b represents middle carbonate cementation; Curve c represents weak carbonate cementation; Curve d represents strong carbonate dissolution; Curve e represents middle carbonate dissolution; Curve f represents weak carbonate dissolution.

porosity reconstructed by feldspar dissolution.  $\partial_5$  is cementation strength, and  $\partial_5 = 0.15$ ,  $\partial_5 = 0.10$ ,  $\partial_5 = 0.025$  represent strong feldspar dissolution, middle feldspar dissolution and weak feldspar dissolution, respectively.

$$V_{Qua\_Dis} = \partial_6 \left( 10 \left( 4.2620 - \frac{5764.2}{T} + \frac{1.7513 \times 10^6}{T^2} - \frac{2.86 \times 10^8}{T^3} \right) \times 10 \left( \left( 2.8454 - \frac{1006.9}{T} + \frac{3.5689 \times 10^5}{T^2} \right) \lg \rho \right) \right) \quad (16)$$

where  $T$  is temperature, °C;  $\rho$  is the density of water, g/cm<sup>3</sup>;  $V_{Qua\_Dis}$  is porosity reconstructed by quartz dissolution.  $\partial_6$  is cementation strength, and  $\partial_6 = 1.2$ ,  $\partial_6 = 1.0$ ,  $\partial_6 = 0.45$  represent strong quartz dissolution, middle quartz dissolution and weak feldspar quartz, respectively.

$$V_{Car\_Dis} = \partial_7 \left( 1.014 \times 10^{-13} X^4 - 1.041 \times 10^{-9} X^3 + 2.636 \times 10^{-6} X^2 + 3.743 \times 10^{-4} X + 0.09743 \right) \quad (17)$$

where  $X$  is burial depth, m;  $V_{Car\_Dis}$  is porosity reconstructed by carbonate dissolution.  $\partial_7$  is dissolution strength, and  $\partial_7 = 2$ ,  $\partial_7 = 1.0$ ,  $\partial_7 = 0.5$  represent strong carbonate dissolution, middle carbonate dissolution and weak carbonate dissolution, respectively.

The present pore volume ( $V_{present}$ ) is calculated using Eq. (18), while the simulation process is described using Fig. 5.

$$V_{present} = V_{primary} + V_{dissolution} - V_{cementation} - V_{compaction} \quad (18)$$

### 3. Results and interpretation

#### 3.1 Diagenetic stages types and its corresponding effect on reservoir evolution

The major diagenetic processes that influence the porosity of the Ed<sub>1</sub> clastic sandstones in the Bozhong depression are mechanical compaction, carbonate cementation, quartz cementation, clay cementation, feldspar dissolution and carbonate dissolution (Table 1). Based on diagenesis of the Ed<sub>1</sub> clastic sandstones and diagenesis models, pore evolution in burial history can be restored (Fig. 8). Meanwhile, data in individual well is for the constraint condition for inversion calculation. In the simulation process, different diagenetic stages have different diagenetic strength, which has a close relationship to diagenetic coefficient  $\partial$ .

The Ed<sub>1</sub> reservoir in the Bozhong depression experienced the process of shallow burial to deep burial (Fig. 6). At the same time, diagenesis intensify from the early diagenetic stage A (IA) to the early diagenetic stage B (IB), and finally to middle diagenetic stage A1 (IIA1) (Fig. 7). The type of diagenesis changed regularly with diagenetic stages. In the early diagenetic stage A, the main diagenesis is mechanical compaction, clay cementation and carbonate cementation. The porosity loss by mechanical compaction, clay cementation and carbonate cementation is ranging from 6.4% ~ 11.8% (av. 9.7%), 2.1% ~ 4.9% (av. 3.5%), 2.6% ~ 6.9% (av.

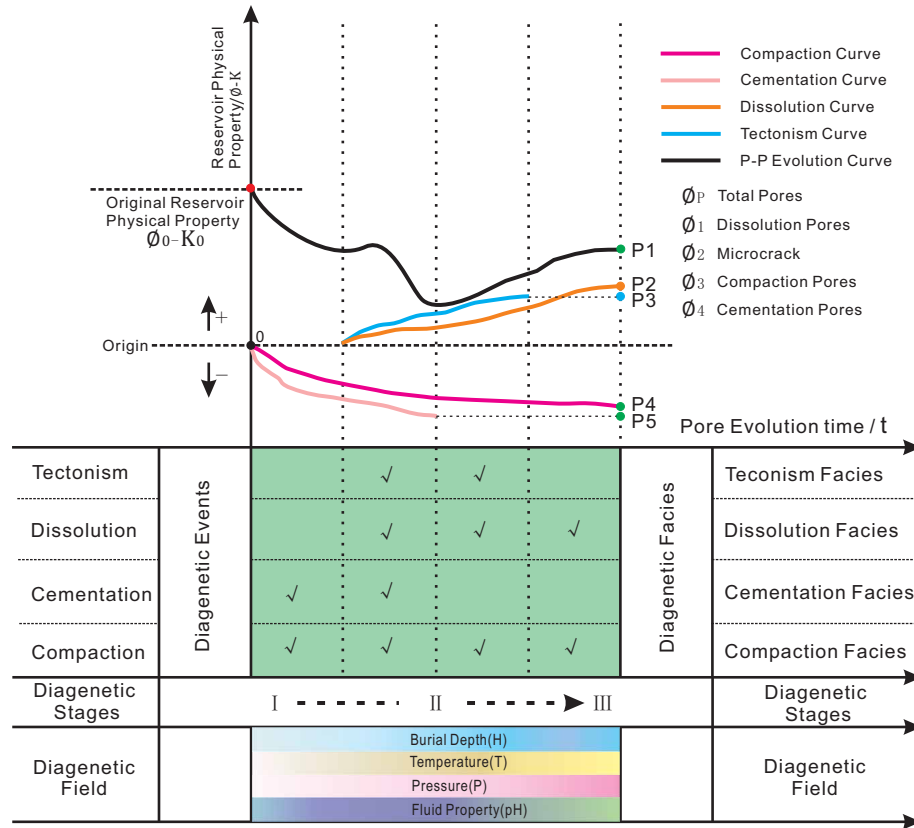


Fig. 5. Simulation of diagenetic stage, diagenesis and porosity evolution.

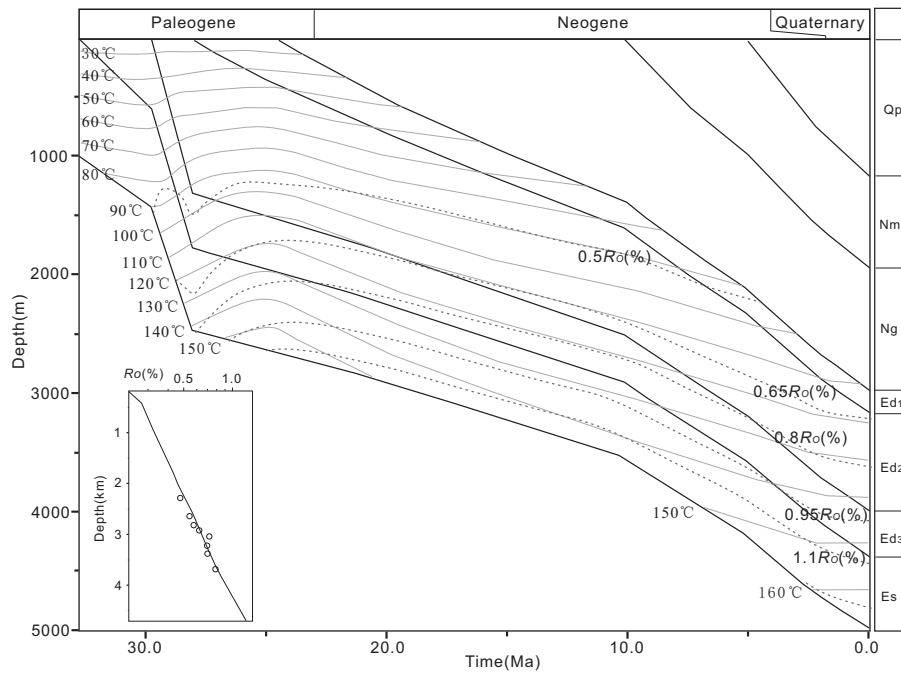


Fig. 6. Burial and thermal modeling of the well ZM4.

5.3%), respectively. In the early diagenetic stage B, the main diagenesis is feldspar dissolution, and the porosity increase by feldspar dissolution is ranging from 0.6% ~ 5.9% (av. 2.5%). In the middle diagenetic stage A1, quartz enlargement and authigenic kaolinite are commonly developed. The main diagenesis types of sandstones in middle diagenetic stage A1 are mechanical compaction and dissolution (Fig. 8).

### 3.2 Evolution of diagenetic facies

Based on Table 3, the type of diagenetic facies also changed regularly with diagenetic stages (Fig. 9). In the early diagenetic stage A, the main diagenetic facies is A-2, clay-B-3, carbonate-B-2 and carbonate-B-3. In the early diagenetic stage B, the main diagenetic facies is A-2, clay-B-2, clay-B-3, carbonate-B-2, carbonate-B-3 and feldspar-C-2. In the middle diagenetic stage A1, the main diagenetic facies is quartz-B-2 and feldspar-C-2. The compaction strength decreases with the buried depth, while the intensity of quartz cementation and feldspar dissolution increases with diagenetic process (Fig. 7). Diagenetic facies is a product of both diagenesis and diagenetic stages under the effect tectonics, which includes rock particles, dissolution, cementation, fabric, pores and cracking. Different diagenetic facies indicates different diagenetic environment and diagenetic process.

## 4. Discussion

### 4.1 Diagenetic evolution sequence

Numerically, diagenesis stage, diagenesis type, and diagenesis sequence are identified to understand diagenesis mode. The main diagenesis types of sandstones in early diagenetic stage A is mechanical compaction, while cementation and dissolution are undeveloped. The main diagenesis types of sandstones in early diagenetic stage B is mechanical compaction, clay cementation, quartz cementation and carbonate cementation, while dissolution is undeveloped. The main diagenesis types of sandstones in middle diagenetic stage A1 is feldspar dissolution and carbonate dissolution, while mechanical compaction and cementation is undeveloped (Fig. 10). Paragenetic sequence of the main diagenetic processes for the Ed<sub>1</sub> reservoir includes middle compaction-weak cementation-weak dissolution, middle compaction-carbonate cementation-weak dissolution and middle compaction-weak cementation-strong dissolution.

Diagenesis is a complex process. The types and intensity of diagenesis are influenced not only by the original material composition but also by the fluid field in different diagenesis stages (Ying et al., 1997; He et al., 2004). For the same diagenesis in the study area, it has different diagenetic evolution sequence in burial process. For example, there are three evolutionary sequences for compaction in the burial history. The first type is medium intensity compaction to medium intensity compaction to medium intensity compaction from early diagenetic stage IA to early diagenetic stage IB to middle diagenetic stage IIA1. The second type is medium intensity compaction to strong intensity compaction to medium intensity

compaction from early diagenetic stage IA to early diagenetic stage IB to middle diagenetic stage IIA1. The third type is strong intensity compaction to medium intensity compaction to medium intensity compaction from early diagenetic stage IA to early diagenetic stage IB to middle diagenetic stage IIA1 (Fig. 10).

### 4.2 Pore evolution model

At present, the numerical simulation methods fall into two major categories. The first category is based on physical or chemical model, which use single factor model to simulate the effect of diagenesis on pores while the other one only considers the comprehensive results of diagenesis on pores, but not caring about concrete diagenesis (Zhang et al., 2013; Wang et al., 2017). In this study the effect of different diagenesis on pores in burial history is firstly simulated, and then a synthetic equation model was established, which can be used to compute the porosity of clastic reservoirs, particularly on reservoirs with low porosity and low permeability. This paper takes the characteristics of present porosity as the cut-in point. The porosity evolution process has two aspects including constructive diagenesis (compaction and cementation) and destructive diagenesis (dissolution), and the two aspects constitute the total porosity evolution process.

Based on diagenesis of the Ed<sub>1</sub> clastic sandstones and diagenesis models, pore evolution in burial history is restored (Fig. 8). Meanwhile, data in individual well is for the constraint condition for inversion calculation. In the simulation process, different diagenetic stages have different diagenetic strength, which has close relationship to diagenetic coefficient  $\partial$ . It is shown that the porosity-permeability-buried depth or porosity-permeability-buried time relationship is non-linear, especially in reservoirs with high diagenesis. Using coefficient  $\partial$  for different diagenetic strength in different diagenetic stages could make the predicted porosities match the measured porosities well.

## 5. Conclusions

A new method is presented for porosity simulation of Ed<sub>1</sub> reservoir in the Bozhong depression. The method is primarily based on the identification of diagenetic stages, diagenesis and its intensity. The workflow of the method is as the following: Firstly, based on previous study and data in individual wells, the diagenetic models are established. Secondly, burial history, paleo temperature and vitrinite reflectivity can be determined using PetroMod 2013 to simulate diagenetic stages evolution in burial history. Thirdly, due to the measured data in individual well including diagenesis and its strength, pore evolution in burial history is simulated. Finally, the reservoirs porosity is predicted accurately without using core data. The method is to predict the reservoir diagenetic of the Ed<sub>1</sub> lake sandstones in the west of Bozhong sag, Bohai Bay Basin.

## Acknowledgments

This research work was funded by Major Projects of Na-



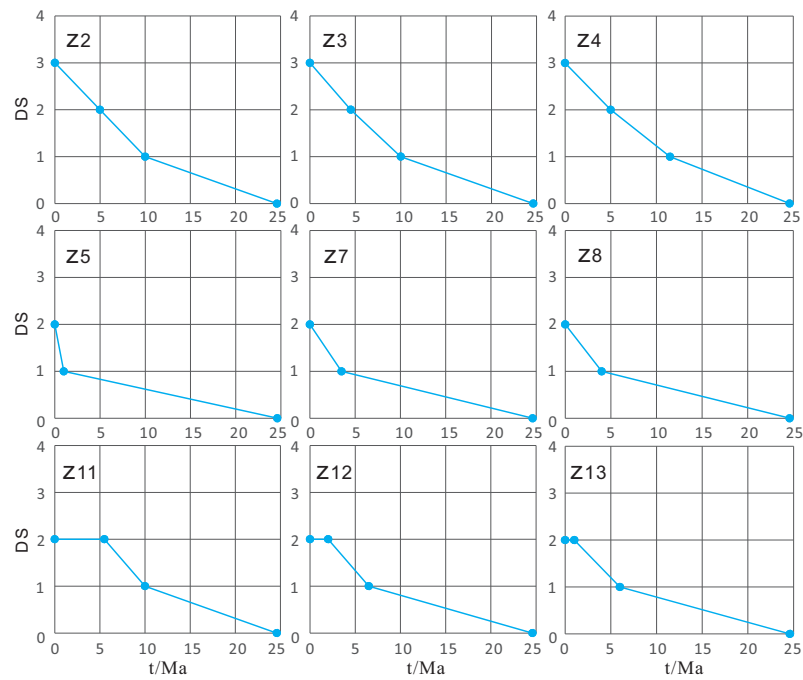


**Fig. 7.** Diagenetic stages (DS) evolution with time. early diagenetic stage A (IA) represented by number 1; early diagenetic stage B (IB) represented by number 2; middle diagenetic stage A1 (IIA1) represented by number 3; middle diagenetic stage A2 (IA2) represented by number 4.

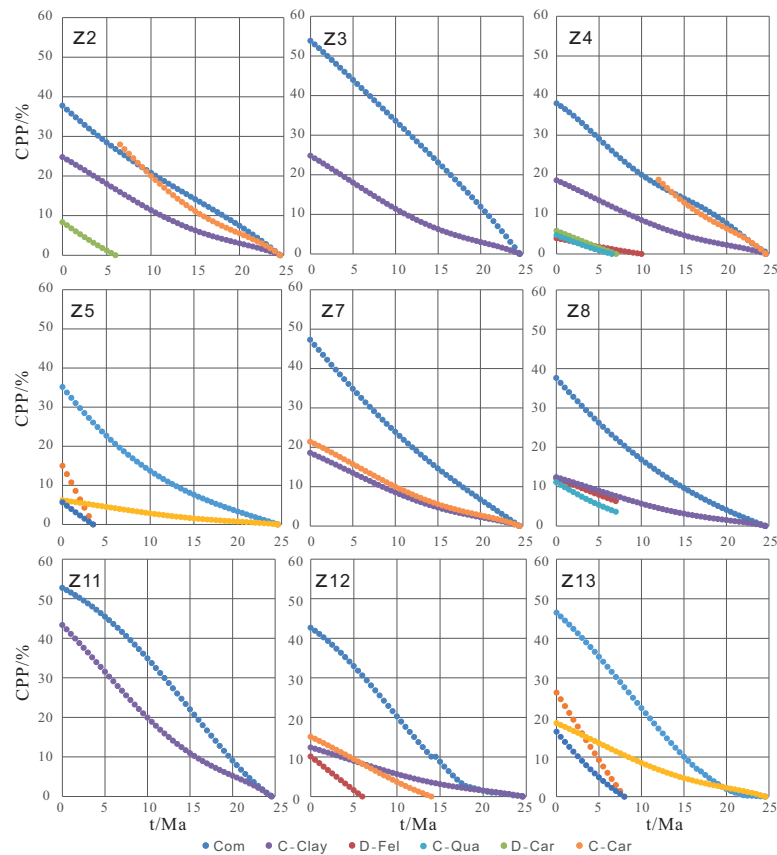


**Fig. 8.** Different diagenesis and its effect on pores evolution in Bozhong depression. CPP is the pore volume destroyed by diagenesis, %; Com is mechanical compaction; C-Clay is clay cementation; D-Fel is feldspar dissolution; C-Qua is quartz cementation; D-Car is carbonate dissolution; C-Car is carbonate cementation.

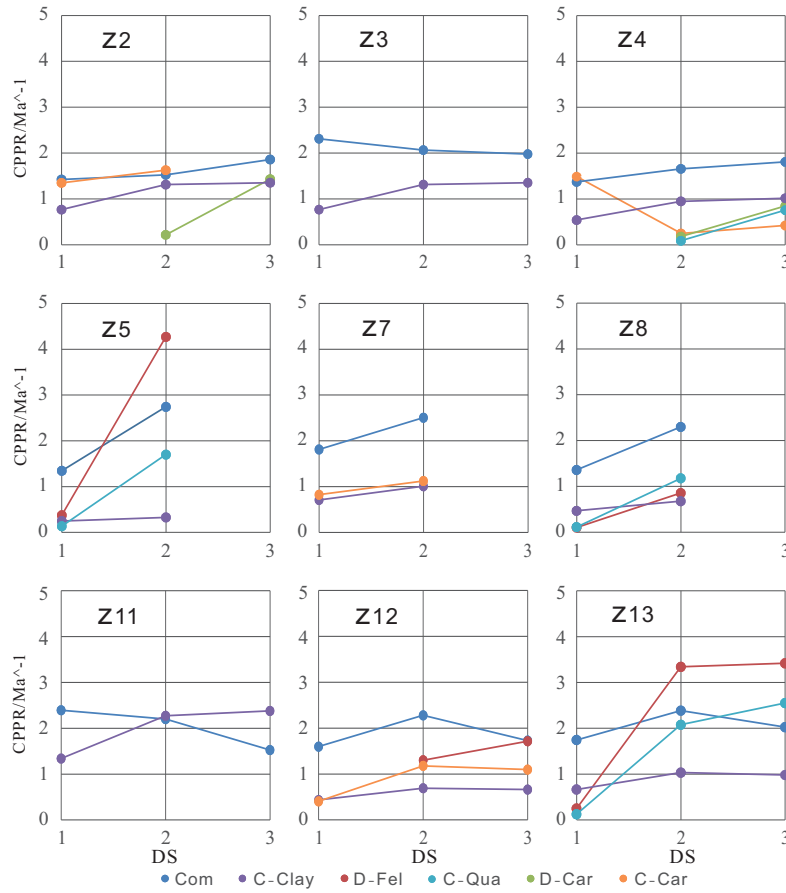


**Fig. 9.** Different diagenesis and its effect on pores evolution in Bozhong depression. Com is mechanical compaction; C-Clay is clay cementation; D-Fel is feldspar dissolution; C-Qua is quartz cementation; D-Car is carbonate dissolution; C-Car is carbonate cementation.

**Table 3.** The classification standard of influence extent on reservoir quality of compaction, cementation and dissolution.

Diagenetic intensity	Compaction facies		Cementation facies (Mono mineral M-j)		Dissolution facies (Mono mineral M-j)	
	Type (A-k)	R-Com	Type (M-B-k)	R-Cem	Type (M-C-k)	R-Dis
Strong	A-1	> 3	M-B-1	> 3	M-C-1	> 3
Medium	A-2	> 1 ~ 3	M-B-2	> 1 ~ 3	M-C-2	> 1 ~ 3
Weak	A-3	> 0 ~ 1	M-B-3	> 0 ~ 1	M-C-3	> 0 ~ 1

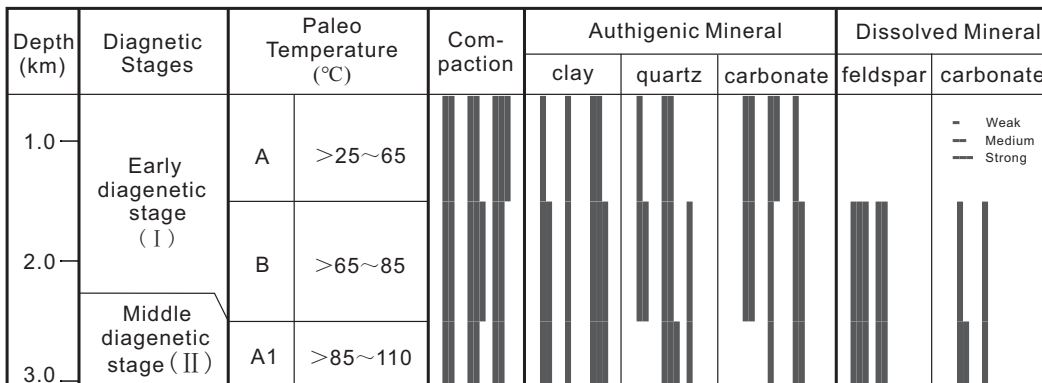


**Fig. 10.** Paragenetic sequence of the main diagenetic processes for the Ed<sub>1</sub> reservoir, based on diagenetic simulation.

tional Science and Technology “Large Oil and Gas Fields and CBM development” (Grant No. 2016ZX05027). Our grateful thanks are due to Shanghai Branch of CNOOC Ltd. for their help in providing geological data. Thanks are also due to anonymous reviewers for their constructive suggestions.

**Open Access** This article is distributed under the terms and conditions of the Creative Commons Attribution (CC BY-NC-ND) license, which permits unrestricted use, distribution, and reproduction in any medium, provided the original work is properly cited.

## References

- Ajdukiewicz, J.M., Nicholson, P.H., et al. Prediction of deep reservoir quality using early diagenetic process models in the Jurassic Norphlet Formation, Gulf of Mexico. *AAPG Bull.* 2010, 94(8): 1189-1227.
- Barker, C.E. Temperature and time in the thermal maturation of sedimentary organic matter. In *Thermal History Of Sedimentary Basins: Methods And Case Histories*, edited by Naeser, N. D., McCulloh, T. H. Springer Science & Business Media, pp: 73-98, 1989.
- Beard, D.C., Weyl, P.K. Influence of texture on porosity and permeability of unconsolidated sand. *AAPG Bull.* 1973, 57(2): 349-369.
- BjØrkum, P.A., Oelkers, E.H., Nadeau, P.H., et al. Porosity prediction in quartzose sandstones as a function of time, temperature, depth, stylolite frequency and hydrocarbon saturation. *AAPG Bull.* 1998, 82(4): 637-648.
- De Segonzac, G.D. The transformation of clay minerals during diagenesis and lowgrade metamorphism: A review. *Sedimentology* 1970, 15(3-4): 281-346.
- Elliot, W.C., Aronson, J.L., Matisoff, G., et al. Kinetics of the smectite to illite transformation in the Denver Basin: Clay mineral, KAr data, and mathematical model results. *AAPG Bull.* 1991, 75(3): 436-462.
- Foscolos, A.E., Powell, T.G., Gunther, P.R., et al. The use of clay minerals and inorganic and organic geochemical indicators for evaluating the degree of diagenesis and oil generating potential of shales. *Geochim. Cosmochim. AC.* 1976, 40(8): 953-966.
- Hao, F., Zou, H., Fang, Y., et al. Kinetics of organic matter maturation and hydrocarbon generation in overpressure environment (in Chinese). *Act. Petrol. Sin.* 2006, 27(5): 9-18.
- He, D., Ying F., Zheng, J., et al. Numerical simulation of clastic diagenesis and its application (in Chinese). *Petrol. Explor. Dev+.* 2004, 31(6): 66-68.
- Jin, Z., Zhu, D., Hu, W., et al. Mesogenetic dissolution of the Middle Ordovician limestone in the Tahe oil field of Tarim Basin, Northwest China. *Mar. Petrol. Geol.* 2009, 26(6): 753-763.
- Lal, D., Chen, J. Cosmic ray labeling of erosion surfaces II: Special cases of exposure histories of boulders, soils and beach terraces. *Earth Planet Sc. Lett.* 2005, 236(3-4): 797-813.
- Lampe, C., Song, G., Cong L., et al. Fault control on hydrocarbon migration and accumulation in the Tertiary Dongying depression, Bohai Basin, China. *AAPG Bull.* 2012, 96(6): 983-1000.
- Lander, R., Walderhaug, O. Predicting porosity through simulating sandstone compaction and quartz cementation. *AAPG Bull.* 1999, 83(3): 433-449.
- Liu, R., Hao, F., Zhu, W., et al. Variation of system openness and geochemical features in overpressured sandstones of the Yinggehai Basin, offshore South China Sea. *Mar. Petrol. Geol.* 2018, 92: 179-192.
- Mahmic, O., Dypvik, H., Hammer, E. Diagenetic influence on reservoir quality evolution, examples from Triassic conglomerates/arenites in the Edvard Grieg field, Norwegian North Sea. *Mari. Petrol. Geol.* 2018, 93: 247-271.
- Marc Audet, D., McConnell, J.D.C., et al. Establishing resolution limits for tectonic subsidence curves by forward basin modelling. *Mar. Petrol. Geol.* 1994, 11(3): 400-411.
- Mashhadi, Z.S., Rabbani, A.R., Kamali, M.R., et al. Burial and thermal maturity modeling of the Middle Cretaceous-Early Miocene petroleum system. Iranian sector of the Persian Gulf. *Petrol. Sci.* 2015, 12(3): 367-390.
- Meng, Y., Huang, W., Wang Y., et al. A kinetic model of clay mineral transformation in overpressure setting and its applications (in Chinese). *Acta Sedimentologica Sinica* 2006, 24(4): 461-467.
- Meng, Y., Jiang, W., Lu, D., et al. Reservoir porosity prediction and its evolving history modeling: A case of Shuang Qing region in the Liaohe west depression. *Acta Sedimentologica Sinica* 2008, 26(5): 780-788.
- Meng, Y., Xu, C., Xie, H., et al. A new kinetic model for authigenic quartz formation under overpressure. *Petrol. Explor. Dev+.* 2013, 40(6): 751-757.
- Morad, S., Ketzer, J.R.M., De Ros, L.F., et al. Spatial and temporal distribution of diagenetic alterations in siliciclastic rocks: Implications for mass transfer in sedimentary basins. *Sediment.* 2000, 47(1): 95-120.
- Mou, Z. A new method to calculate the ancient thickness of sedimentary sequences (in Chinese). *Petroleum Geology & Expeximent* 1993, 15(4): 414-422.
- O’Sullivan, M.J., Pruess, K., Lippmann, M.J. State of the art of geothermal reservoir simulation. *Geothermics* 2001, 30(4): 395-429.
- Price, L.C. Geologic time as a parameter in organic metamorphism and vitrinite reflectance as an absolute paleogeothermometer. *J. Petrol. Geol.* 1983, 6(1): 5-37.
- Pytte, A.M., Reynolds, R.C. The thermal transformation of smectite to illite, in *Thermal History of Sedimentary Basins*, edited by Naeser, N.D., McCulloh, T.H. Springer Science & Business Media, pp: 133-140, 1989.
- Qian, W., Yin, T., Zhang, C., et al. Forming condition and geology prediction techniques of deep clastic reservoirs. *Acta Geol. Sin.-Engl.* 91 (supp.1). 2017, 91(s1): 255-256.
- Schmoker, J.W., Gautier, D.L. Sandstone porosity as a function of thermal maturity. *Geology* 1988, 16(11): 1007-1010.
- Shi, G.R. Numerical methods of petroliferous basin modeling, 3rd edn. Petroleum Industry Press, Beijing, 2005.
- Sweeney, J.J., Burnham, A.K. Evaluation of a simple model of vitrinite reflectance based on chemical kinetics. *AAPG Bull.* 1990, 74(10): 1559-1570.

- Taylor, T.R., Giles, M.R., Hathon, L.A., et al. Sandstone diagenesis and reservoir quality prediction: Models, myths, and reality. *AAPG Bull.* 2010, 94(8): 1093-1132.
- Tobin, R.C. Porosity prediction in frontier basins: A systematic approach to estimating subsurface reservoir quality from outcrop samples. *AAPG Memori* 69 1997: 1-18.
- Tribble, J.S., Arvidson, R.S., Lane III, M. Crystal chemistry, and thermodynamic and kinetic properties of calcite, dolomite, apatite and biogenic silica: Applications to petrologic problems. *Sediment. Geol.* 1995, 95(1-2): 11-37.
- Walderhaug, O. Kinetic modeling of quartz cementation and porosity loss in deeply buried sandstone reservoirs. *AAPG Bull.* 1996, 80(5): 731-745.
- Wang, J., Cao, Y., Liu, K., et al. Identification of sedimentary-diagenetic facies and reservoir porosity and permeability prediction: An example from the Eocene beach-bar sandstone in the Dongying Depression, China. *Mar. Petrol. Geol.* 2017, 82: 69-84.
- Williams, R.T., Farver, J.R., Onasch, C.M., et al. An experimental investigation of the role of microfracture surfaces in controlling quartz precipitation rate: Applications to fault zone diagenesis. *J. Struct. Geol.* 2015, 74: 24-30.
- Wilson, M.D., Stanton, P.T. Diagenetic mechanisms of porosity and permeability reduction and enhancement. *Special Publications of SEPM* 1994, 78: 59-118.
- Wood, J.R., Byrnes, A.P. Alternate and emerging methodologies in geochemical and empirical modeling. *Special Publications of SEPM* 1994, 30: 395-400.
- Xu, D., Wang, Y., Han, X. Experimental method for quantitative characterization of apparent compaction rate and apparent cementation rate (in Chinese). *Pro. Geophy.* 2018, 33(01): 274-278.
- Yang, N., Wang, G., Lai, J., et al. A method for calculation primary porosity of sandstone. *Geophysical and Geochemical Exploration* 2013, 37(4): 726-729.
- Ying, F., He, D., Long, Y., et al. The division of diagenetic stages in clastic rocks (SY/T 5477-2003) (in Chinese), 2003.
- Yuan, G., Cao, Y., Gluyas, J., et al. Reactive transport modeling of coupled feldspar dissolution and secondary mineral precipitation and its implication for diagenetic interaction in sandstones. *Geochim. Cosmochim. Ac.* 2017, 207: 232-255.
- Zheng, J., Ying, F. Diagenetic sequence and model of reservoirs of coal-bearing formation for prediction oil and gas distribution (in Chinese). *Petrol. Scien. Tech. P.* 1997, 4: 19-24.